タイトル	Quantitative Mathematical Analysis of Thyroid Ultrasonography Using Fractal Dimension
作成者（著者）	Komatsu, Fumiya / Kijima, Sho / Kawagoe, Naoyuki / Maruyama, Kenichi / Tsuboi, Kumiko / Urita, Yoshihisa
公開者	The Medical Society of Toho University
発行日	2020.03.01
ISSN	21891990
掲載情報	Toho Journal of Medicine. 6(1). p.20-29.
資料種別	学術雑誌論文
内容記述	Original Article
著者版フラグ	publisher
JaLCDOI	info:doi/10.14994/tohojmed.2019-012
メタデータのＵＲＬ	https://mylibrary.toho-u.ac.jp/webopac/TD14112953

Original Article

Quantitative Mathematical Analysis of Thyroid Ultrasonography Using Fractal Dimension

Fumiya Komatsu[1)]* Sho Kijima[2)] Naoyuki Kawagoe[3)]
Kenichi Maruyama[4)] Kumiko Tsuboi[5)] and Yoshihisa Urita[2)]

[1)]Department of general medicine and emergency care, Toho University Graduate School of Medicine, Tokyo, Japan
[2)]Department of general medicine and emergency care, Toho University Omori Medical center, Tokyo, Japan
[3)]Division of Diabetes, Metabolism, and Endocrinology, Department of Internal Medicine, Toho University Sakura Medical center, Chiba, Japan
[4)]Department of Clinical Functional Physiology, Toho University Omori Medical center, Tokyo, Japan
[5)]Division of Diabetes, Metabolism, and Endocrinology, Department of Internal Medicine, Toho University Omori Medical center, Tokyo, Japan

ABSTRACT

Introduction: On the basis of the self-similarity of the human body, fractal dimensions can be calculated mathematically. Fractal analysis can also quantitatively express the density and complexity of a structure as a fractal dimension. We hypothesize that the fractal dimensions of ultrasonographic findings would change in thyroid disease. In this study, we explore the possibility of applying fractal analysis to the quantitative evaluation of ultrasonographic findings in thyroid tissue.

Methods: This retrospective study used data on 1205 patients who newly received thyroid ultrasonography between April 2004 and March 2016. Patients who were included had one or more of the following: normal thyroid, Graves' disease, Hashimoto's thyroiditis, subacute thyroiditis, adenomatous goiter, or papillary carcinoma. Furthermore, the fractal dimension of thyroid ultrasonography was calculated in sagittal pictures. The region of interest was set along the contour of the thyroid gland, excluding a film. Fractal analysis was performed using box-counting methods.

Results: For the normal thyroid gland, there was a significant decrease in the fractal dimensions of both contour and concentration structures, with significant differences compared with the disease groups. Among the thyroid disease groups, papillary carcinoma had the highest fractal dimension. The fractal dimension of the thyroid gland increased with age in the normal group. There were no differences in fractal dimensions by gender.

Conclusion: Fractal analysis makes it possible to objectively determine the presence of chronic inflammation in thyroid tissue, but it is difficult to distinguish papillary carcinoma from benign goiter.

Toho J Med 6 (1): 20–29, 2020

*Corresponding Author: Fumiya Komatsu, 6-11-1 Omorinishi, Ota-ku, Tokyo 143-8541, Japan, tel: 03–3762–4151
e-mail: fumiya.komatsu@med.toho-u.ac.jp
DOI: 10.14994/tohojmed.2019-012

Received June 13, 2019: Accepted Sept. 2, 2019
Toho Journal of Medicine 6 (1), Mar. 1, 2020.
ISSN 2189–1990, CODEN: TJMOA2

KEYWORDS: thyroid ultrasonography, fractal dimension, adenomatous goiter, papillary carcinoma

Introduction

Ultrasonographic examination is clinically useful in many aspects of thyroid disease management, including echogenicity, nodularity, and size measurement. The alterations in thyroid structure in ultrasonography (US), such as nodules, are most often characterized by size, irregular margins, microcalcifications, and central vascularity even though the information obtained from ultrasonographic findings is hidden in the complexity of the thyroid gland structure. The lack of objectivity in the interpretation of ultrasonographic findings might lead to important information being overlooked (e.g., information that could be useful in evaluating the severity of inflammation, the magnitude of the structure destroyed, and the influence of dietary iodine intake). Furthermore, the diagnostic performance of US is highly affected by subjectivity with interobserver and intraobserver variability. To overcome such limitations, quantitative analyzes are used for objective interpretation. Euclidean geometry is routinely used in analyzing medical images to distinguish gross differences even though it is unable to quantitatively evaluate the complexity.

For fractals, Mandelbrot[1] advocated self-similar features in 1958 as fractals. Fractals can exploit the self-similarity and express the density and complexity of objects as a fractal dimension. In nature, we often see objects with self-similarity, such as branching trees or rias-style coastlines. The self-similarity of the human body, which results from self-organization, is found in bronchial branches and artery networks.[2] When a structure is unable to maintain self-similarity, its fractal dimension should change.

Several methods can be used to perform quantitative morphologic analyzes in medical images. Fractal analysis is one of the methods that utilize self-similarity and quantitatively evaluate complicated forms as fractal dimensions.[2] It seems to have great potential in the medical image analysis of complicated forms because the borders of some natural objects, including the human body, could be fractal. A fractal dimension is a noninteger value related to the relationship between the measured metric and the scale used.

There are several studies on other organs associated with fractal dimensions. To evaluate the malignant potential of nodules, fractal dimensions were calculated from the digital nuclear images of biopsy specimens obtained from various diseases, including epidermal changes associated with HPV virus infection,[3] oral squamous cell carcinoma,[4] laryngeal carcinoma,[5] multiple myeloma,[6] malignant melanoma,[7] colorectal cancer,[8] prostate cancer,[9] endometriosis and endometrial adenocarcinoma,[10] and acute precursor B lymphoblastic leukemia.[11] The studies revealed a correlation between a higher fractal dimension and a shortening of survival time, thus suggesting the possibilities of using fractal dimension as a predictor of prognosis. On the basis of the theory that fractal dimension represents a quantitative characteristic to describe morphological complexity and provides information on the self-similarity properties of the shape,[1] it can be said that the structure of malignant neoplasmas becomes more complex. The same explanation is also consistent with the results of an endoscopic study. Sato[12] analyzed the pit patterns of colonic epithelial neoplasia by using endoscopy and revealed the close association between increased fractal dimension and higher malignant potential.

We hypothesize that the fractal dimensions of ultrasonographic findings would differ in thyroid disease from those in normal thyroid tissue. In this study, we explore the possibility of applying fractal analysis to the quantitative evaluation of ultrasonographic findings in thyroid tissue. Furthermore, to more accurately and subjectively distinguish various diseases and normal thyroid images, we propose the fractal analysis of thyroid ultrasound images.

Methods

1. Principle of fractal analysis

Mandelbrot proposed the concept of a fractal, which is a generic term for figures and structures that have self-similarity. Self-similarity is a property indicating that when a part of a figure is expanded, the form matches the whole or another part. Fractals show uniform self-similarity with the same structure when expanding details in any part.[1] From this feature, it is used as a method to understand the complexity of an object. The same structure as the whole cannot be regarded a surface (two dimensions) no matter how large it is expanded and no matter where it is expanded. Furthermore, it cannot be considered a line (one dimension). In other words, the dimen-

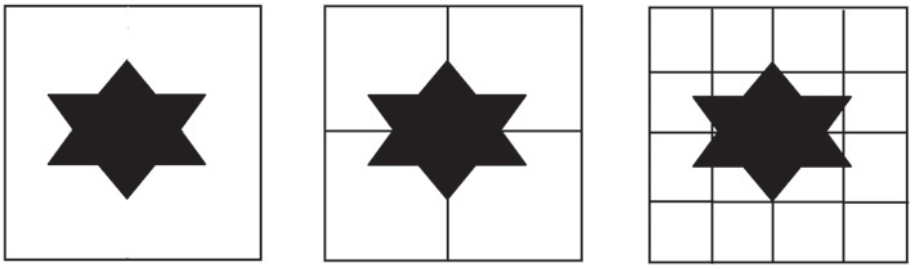

Fig. 1 Principle of box-counting methods. The whole object is covered by a box that is divided into two equal parts. As mentioned above, a box containing the target and a box not containing are present. Count the boxes containing the object and compare it with the number of whole boxes.

sion of the fractal structure cannot be represented by an integer. The dimension can be calculated from the feature of this similarity. The methods for calculating the dimension are shown below.

When a line segment is divided into two equal parts, there are two-line segments of similar figures. In the case of a square, dividing each side into two equal parts divides the square into four similar squares. Similarly, a cube is divided into eight similar cubes. If these are expressed as power functions in order, they are $2 = 2^1$, $4 = 2^2$, and $8 = 2^3$. The multiplier of the power function matches the dimension of the figure, and it is possible to write $b = a^D$ when equally dividing a line segment into 1/a and when obtaining b similar figures. This value D is defined as the fractal dimension. If this function is represented logarithmically (i.e., logb = Dloga), then D = logb / loga is the similarity dimension.[1] However, this method has a limitation: only objects with fractal structures can be calculated.

Natural objects do not exhibit perfect fractal structures. Although there are various methods for determining the dimension of the fractal structure, such as similarity dimension, divider dimension, pixel dilation dimension, Hausdorff dimension, and box-counting dimension, the most commonly used dimension in biological science is the box-counting dimension. This dimension is calculated by box-counting methods, which can also be used to calculate objects without fractal structures. This method was defined by Russel et al.[13, 14]

The box-counting principle is based on counting the number of boxes of various side lengths needed to cover the surface of objects (Fig. 1).[2, 14–16] The number of boxes is counted in each side length. When a side length is divided into two equal parts, four squares are needed to cover the object and to surround the binary object with a square. Ten boxes are needed when using a side length of one-fourth. This process is repeated with grids comprising boxes of varying side lengths. The log of the number of boxes needed to cover the object is plotted against the log of a reciprocal number of the side length. The slope of the resulting line is defined as a fractal dimension.

2. Data acquisition

The study protocol was approved by the Ethics Committee of Toho University Omori Medical Center (No. M 1808817017). The US images of 1205 patients suspected for thyroid diseases were collected from the database of Toho University Omori Medical center between April 2004 and March 2016. Patients were classified into six groups according to ultrasonographic findings (Table 1). Among these patients, 28 patients (2.3%) were histologically diagnosed with papillary carcinoma: 21 female patients and seven male patients (mean age of 52.8 years). Graves' disease and Hashimoto's thyroiditis were diagnosed on the basis of the diagnostic criteria.[17]

The mean ages of patients with subacute thyroiditis and Hashimoto's thyroiditis were 46.1 and 54.7 years, respectively. Graves' disease and adenomatous goiter had mean ages of 48.2 and 59.8 years, respectively. Women comprised more than 70 percent of patients in all groups. Subjects with normal blood levels of thyroid hormone and without abnormal US findings were classified into the normal group (290 female and 121 male subjects with a mean age of 48.1 years). Patients with a past history of thyroidectomy were excluded from the analyzes.

Table 1 Comparison of the Characteristics between Normal Thyroid and Patient Groups

	Normal thyroid	Subacute thyroiditis	Hashimoto's thyroiditis	Graves' disease	Adenomatous goiter	Papillary carcinoma
No	411	28	248	62	335	28
Mean age (y)	47.2	46.1	54.7	48.2	59.8	52.8
Sex						
Male	132	5	44	18	66	7
Female	330	23	231	52	276	21

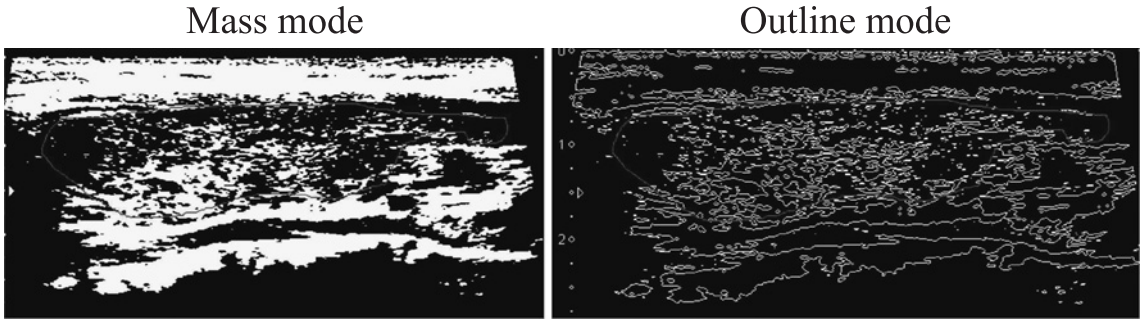

Fig. 2 Sample images of Mass mode and Outline mode.
ROIs were drawn along the contour of the thyroid gland. The figure on the left is imaged by Mass mode, and the figure on the right is imaged by Outline mode.
Mass mode is defined as the maximum value obtained by setting the density threshold. Outline mode emphasizes the outline of the object and is obtained by analyzing the complexity of the real outline.

3. Measurement of fractal dimension

Longitudinal grayscale US images that used an 8-10 MHz linear array transducer were selected. Subsequently, the regions of interest (ROIs) were drawn along the contour of the thyroid gland, excluding the film (Fig. 2). If nodules were located only in the mate of thyroid lobes, they were drawn on the lobe with nodules. The right lobe was selected in subjects without abnormal findings and in patients with nodules at both lobes. The equipment used was HI VISION Preirus (Hitachi Medical Systems, Tokyo, Japan); SSA-770A, SSA-700A, or TUS-A 500 (Canon Medical Systems, Tokyo, Japan); or the Aplio 500 ultrasound system (Toshiba Medical Systems, Tokyo, Japan).

All US image extractions were implemented by fractal analysis software (custom fractal version 1.00; DBkids, popimaging, Kanagawa, Japan).

Thyroid ultrasound images were captured in analysis software and converted to grayscale for use. Two kinds of fractal dimensions were calculated by the box-counting method: Mass mode, which is defined as a maximum value obtained by setting the density threshold at 10% increments (Fig. 2, left side), and Outline mode, which is obtained by using two neighboring thresholds to emphasize the outline of an object and to analyze the complexity of parenchymal contours (Fig. 2, right side).

4. Statistical analysis

All statistical analyzes were performed with easy R (EZR) (Saitama Medical Center, Jichi Medical University, Saitama, Japan), which is a graphical user interface for R (The R Foundation for Statistical Computing, Vienna, Austria). We used the nonparametric Kruskal-Wallis test, Steel-Dwass test, and Mann-Whitney U test to compare the fractal dimensions between groups. $P < 0.05$ was regarded significant.

Results

1. Fractal dimension in each thyroid disease

Table 2 shows the fractal dimensions calculated by Mass mode and Outline mode. Calculation by both modes revealed that the mean fractal dimension was the lowest in normal thyroid. Among patients with nodules, the US images of papillary carcinoma had the highest fractal dimension, followed by adenomatous goiter in Mass mode. In Outline mode, the second highest fractal dimension was observed in inflammatory disease. There is no significant difference between papillary carcinoma and adenomatous

Table 2 Results of Calculating the Fractal Dimension by Using Mass Mode and Outline Mode

	Mass mode mean [95%CI]	Outline mode mean [95%CI]
Normal thyroid	1.510492 [1.500252-1.520732]	1.296627 [1.286645-1.306609]
Subacute thyroiditis	1.582810 [1.537338-1.628283]	1.351847 [1.316821-1.386873]
Hashimoto's thyroiditis	1.563782 [1.551165-1.576400]	1.355510 [1.344650-1.366370]
Graves' disease	1.599033 [1.578080-1.619986]	1.395345 [1.377594-1.413097]
Adenomatous goiter	1.582762 [1.570531-1.594993]	1.349947 [1.338878-1.361017]
Papillary carcinoma	1.688304 [1.641269-1.735339]	1.411520 [1.370191-1.452850]

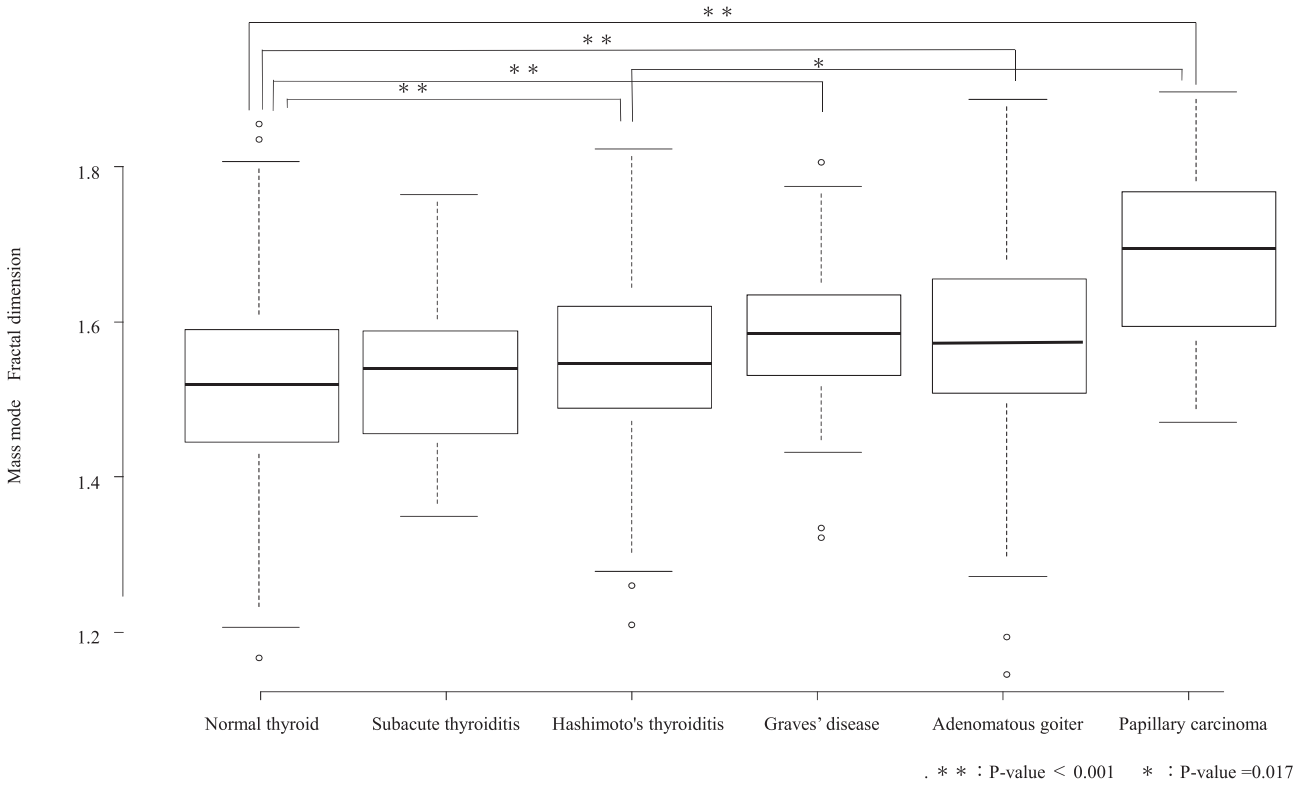

Fig. 3 Comparison of fractal dimensions between each group calculated by Mass mode.
Normal thyroid had significantly lower values of fractal dimension than adenomatous goiter, papillary carcinoma, Hashimoto's thyroiditis, and Graves' disease. However, there was a significant difference in the fractal dimension of US images between papillary carcinoma and Hashimoto's thyroiditis.

goiter. However, the difference from normal is largest between papillary carcinoma and adenomatous goiter. The fractal dimensions in each diffuse thyroid disease was higher than that in normal thyroid, and the parenchymal image of thyroid in Graves' disease had the highest fractal dimension, followed by subacute thyroiditis and Hashimoto's thyroiditis.

Compared with normal thyroid images, the fractal dimensions in papillary carcinoma, Graves' disease, adenomatous goiter, and Hashimoto's thyroiditis were significantly higher than those in Mass mode (Fig. 3) and Outline mode (Fig. 4). There was a significant difference in the fractal dimension of US images between thyroid and Hashimoto's thyroiditis only in Mass mode. The parenchymal image of thyroid in subacute thyroiditis had higher fractal dimensions than that of normal thyroid, but the differences did not reach a statistical significance in Mass mode or Outline mode.

2. Changes in fractal dimension by age and sex

The relationship between age and fractal dimension of thyroid parenchyma on US in Mass mode (Fig. 5) demonstrated that these values increased with age in a nearly

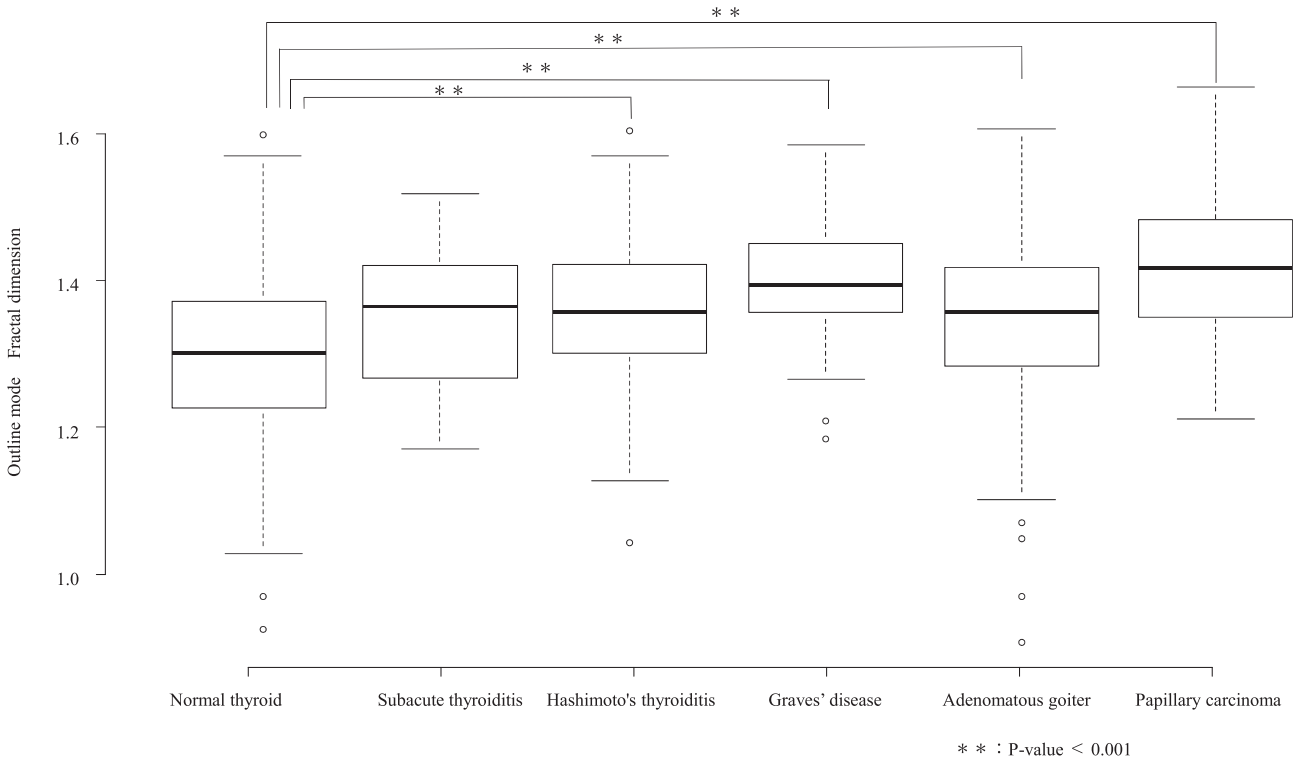

Fig. 4 Comparison of fractal dimensions between each group calculated by Outline mode.
Normal thyroid had significantly lower values of fractal dimension than adenomatous goiter, carcinoma, Hashimoto's thyroiditis, and Graves' disease. Papillary carcinoma had the highest fractal dimension.

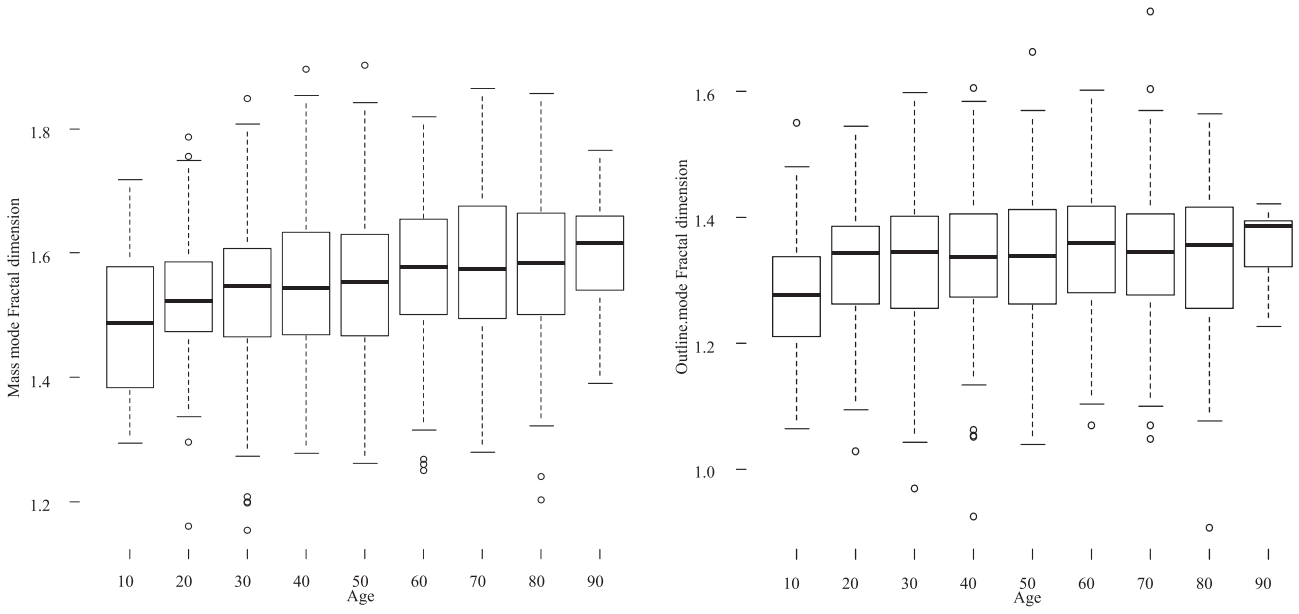

Fig. 5 Relationship between age and fractal dimension calculated by Mass mode and Outline mode. The age ranges plotted are 15-19, 20-29, 30-39, 40-49, 50-59, 60-69, 70-79, 80-89, and＞90 years. Fractal dimension increased with age ($p<0.001$).

linear fashion: from 1.487141 in those aged 15-19 years to 1.616446 in those aged 80-89 years. In Outline mode, an age-dependent increase was noted in the fractal dimensions (Fig. 6).

Fig. 6 shows the relationship between sex and each fractal dimension. The mean fractal dimensions of thyroid parenchymal images in Mass mode obtained by US were 1.553038±0.082742 in females and 1.566234±0.069291 in

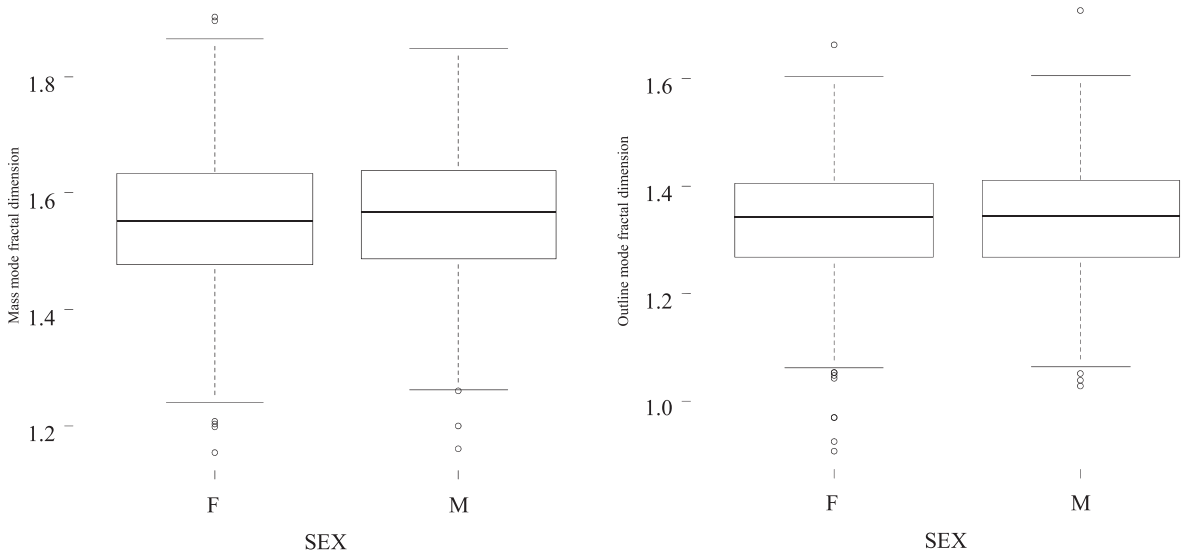

Fig. 6 Fractal dimensions in Mass mode and Outline mode by gender.
There were no significant differences in fractal dimensions between female and male subjects.

males, whereas these values in Outline mode were 1.344102±0.062182 in females and 1.344834±0.077382 in males. There were no significant differences in fractal dimensions between female and male subjects in the two modes.

Discussion

US diagnoses based on the visual inspection of images are dependent on a performer with interobserver and intraobserver variations in the evaluation of diffuse thyroid diseases both with and without nodules. To overcome the limitations, quantitative analysis was performed with a histogram and gray level co-occurrence matrix.[18–20] Quantitative analysis assists clinical physicians in facilitating the accurate and fast classification of benign and malignant thyroid nodules, thus avoiding unnecessary biopsies for adenomatous goiter.

According to the results of this study, the fractal dimension calculated by both Mass mode and Outline mode increased in the disease group. Papillary carcinoma had the highest fractal dimension, thus suggesting that the US images of papillary carcinoma have the most complex structure because the fractal dimension is larger if the border of the object is more rugged, its lines more irregular, and its branching pattern more abundant. Ferreira et al.[21] reported the usefulness of fractal dimensions for the pathological diagnosis of thyroid follicular neoplasias. Therefore, quantitative analyzes may provide additional information that is invisible to the human eye. Prochazka et al.[22] recently gathered the published studies of quantitative analyzes for the US images of thyroid nodules. However, there are few studies on quantitative analyzes for the US images of diffuse thyroid disease.

There are several studies on fractal analyzes using radiological imaging. The implementation of fractal analysis detects clinically relevant changes during lung cancer development in computed tomography images.[23] Sequential computed tomography images were taken from a patient who declined treatment for the diagnosed stage I adenocarcinoma of the lung. Progressive tumor growth and changes in shape over five years based on cancer progression were demonstrated in that case. The fractal dimension increased from 1.4095 to 1.6250 during the five-year period. Al-Kadi and Watson revealed that the fractal dimension of lung tumor tissue was higher than that of normal lung tissue and that more aggressive tumors (stages III-IV) had a higher fractal dimension than nonaggressive tumors (stage I). Hayano et al.[24] reported that patients with tumors presenting a lower fractal dimension on the arterial phase image at baseline showed longer progression-free survival, whereas tumor density and size showed no significant correlations with progression-free survival. A higher fractal dimension was associated with a higher malignant potential; this finding is consistent with our results that the US images of papillary carcinoma had the highest fractal dimension, followed by adenomatous goiter. There was no significant difference in fractal dimension between papillary carcinoma and adenomatous

goiter.

In clinical practice, nodules suspicious of malignancy are examined histologically by fine needle aspiration cytology (FNAC) to distinguish between adenomatous goiter and thyroid cancer. FNAC was often repeated to the physicians' satisfaction until the nodule was accurately determined as showing no malignancy. As shown in the results of this study, additional analyzes by fractal dimension could assist physicians in diagnosing thyroid nodules and in avoiding unnecessary FNAC.

Thyroid tissue consists of thyroid follicular epithelial cells, which secrete thyroid hormone and thyroid follicles.[25, 26] In the results of this study, both fractal dimension Mass mode and fractal dimension Outline mode showed elevations with significant differences in Graves' disease. The increased fractal dimension reflects a dense structure in Mass mode and the complexity of borders in Outline mode. It is possible that an increased fractal dimension in Graves' disease results from the active proliferation of follicular cells, enrichment of blood stream, infiltration of various inflammatory cells, and/or an overproduction of thyroid hormones. Homogeneous parenchymal echogenicity on US reflects a dense structure consisting of various cells of similar ratios because echogenicity is produced by differences in ultrasonic impedance. It is suggested that the fractal dimension of thyroid ultrasound images also reflects the quantitative damage of inflammatory thyroid diseases.

The parenchymal image of the thyroid in subacute thyroiditis, which often has marked inflammation, had higher fractal dimensions than that in normal thyroid, but there was no significant difference in Mass mode or Outline mode. Although this is mainly due to the lack of patients with subacute thyroiditis, it is also caused by the minute-by-minute changes in ultrasound findings. Ultrasound findings in the acute phase include irregular and ill-defined hypoechogenic areas, predominantly in the subcapsular region, whereas ultrasound findings in the subacute phase progress to a more diffuse pattern with pseudonodular formation.[27] This rapid progress of thyroiditis leads to varied findings depending on the timing of ultrasound examination.

When sound passing through a totally homogeneous medium does not encounter interfaces to reflect sound, the medium appears anechoic. There is a junction of materials with different physical properties and acoustic interfaces, which are responsible for the reflection of variable amounts of the incident sound energy.[25] When ultrasound passes from one tissue to another, different acoustic impedances are reflected. The amount of reflection is determined by the difference in the acoustic impedances of tissues forming the interface. Interfaces composed of tissues with small differences in acoustic impedance reflect only part of the incident energy, whereas those with large acoustic impedance differences reflect almost all the incident energy.

Thyroid parenchyma has medium- to high-level echogenicity. Muller et al.[26] reported that the mean follicle lumen diameter in thyroid structures diagnosed as normal by using a 5 MHz transducer was 67 μm. By applying this information to a 7.5 MHz transducer, we find that a homogeneous thyroid parenchyma accounts for the interfaces that are uniformly distributed and that the size is more than 100 μm. The cause for sound reflection is the difference in acoustic impedance at the boundary of two media: a high colloid content and a relatively low cellular portion. A large proportion of sound waves hits the cell-colloid interface and is reflected back to the transducer without scattering, thus resulting in homogeneous pictures with moderate echogenicity. In the case of microfollicular or follicle-free tissue, a small proportion of sound waves hits the acoustic interface, thus resulting in low-echogenic pictures. Thyroid tissue with increased cellularity and decreased follicles has fewer acoustic interfaces. This histological change should lead to lower echogenicity but also increases the complexity of a structure. Considering that thyroid malignancies are not uniform normofollicular structures, the US images of papillary carcinoma had the highest fractal dimension to reflect increased the complexity of the acoustic interface.

Although thyroid disorders and thyroid diseases are reported to increase with advancing age,[28, 29] it is not clear whether US images change with altered thyroid function. The reduction in the weight of the gland, the volume of follicles, the content of colloid, and the proliferation of connective tissue associated with aging suggest a reduction in the activity of the gland.[30] Decreased follicles in the thyroid gland with age lead to the increased number of cell-colloid interface, which is the main cause of acoustic reflection, thus resulting in higher fractal dimensions in the elderly.

This study showed that fractal dimensions increase with age, but there are no significant differences in fractal dimension by gender; moreover, males are highly corre-

lated with the risk and aggressiveness of papillary carcinoma.[19] The increased fractal dimensions found in the elderly are considered the result of a changed structure due to increased heteromorphism and atrophic changes of the thyroid gland. Further histological studies are needed to clarify the association between increased fractal dimension and aging.

Considering that fractal analysis is unaffected by image magnification, this type of analysis is suitable for a retrospective study using previously obtained medical images.[31] However, there are some limitations to this study. First, fractal analysis is a morphological method. It is unclear whether a change in fractal dimension reflects the functional disorders of the thyroid gland. Further studies are needed to evaluate the association between fractal dimension and thyroid function. Second, ultrasonographic examination was not always performed with the same equipment. Different types of equipment might have caused variance in the calculation of fractal dimension, even in the same individual. Third, the absolute value of the fractal dimension varies depending on the calculation method. The validity of the box-counting method used to calculate the fractal dimension in the present study was found by Russell[5] as described above and is used as the most general calculation method for the fractal dimension. However, some restrictions have been indicated, such as the discovery of self-similarity and sensitivity to the size of the box.[32–34] Fourth, the longitudinal changes of the fractal dimension might be found in inflammatory thyroid diseases. Repeated examinations would present the time course of morphological and functional changes in thyroid diseases.

Finally, there are concerns about measurement errors owing to differences in the measurement equipment used because the following vary widely: distance between the surface of the probe and ROI; the subcutaneous fat thickness; the magnitude of the reflected signal, which depends on the depth of penetration; and time gain control in ultrasound application.[35] In general, the fractal dimension is not influenced by magnification rate because fractals can be any type of infinitely scaled and repeated pattern. Although the resolution of US relies on the frequency range used, the gain of the measurement signal input section, and the cutoff frequency of the external filter, the optical density of ultrasonic pictures is adjusted for analysis by selecting the maximal fractal dimension at each measurement. This process can overcome the difference in measurement equipment for the most part.

In summary, fractal analysis makes it possible to objectively decide the presence of chronic inflammation in thyroid tissue. Contrary to our expectations, it is difficult to clearly distinguish papillary carcinoma from benign goiter even by using a fractal dimension, although the US images of papillary carcinoma had the highest fractal dimension. Further studies in the greater number of patients with papillary carcinoma may be able to discriminate between malignant and benign goiters. A novel quantitative diagnostic method independent of interobserver variation could lead to automatic diagnosis in the future.

Acknowledgements: This study did not receive any specific grants from funding agencies. The Excel file data used to support the findings of this study are available from the corresponding author upon request.

Conflicts of interest: None declared.

References

1) Mandelbrot BB. The fractal geometry of nature. 2nd ed. New York: W. H. Freeman and Company; 1982.
2) Manuel V, Raul R-E, Maria JMDJ. Chaos, Fractals, and Our Concept of Disease. Perspect Biol Med. 2010; 53: 584-95.
3) Ahammer H, Kroepfl JM, Hackl C, Sedivy R. Fractal dimension and image statistics of anal intraepithelial neoplasia. Chaos, Solitons and Fractals. 2011; 44: 86-92.
4) Bose P, Brockton NT, Guggisberg K, Nakoneshny SC, Kornaga E, Klimowicz AC, et al. Fractal analysis of nuclear histology integrates tumor and stromal features into a single prognostic factor of the oral cancer microenvironment. BMC Cancer. 2015; 15: 409.
5) Delides A, Panayiotides I, Alegakis A, Kyroudi A, Banis C, Pavlaki A, et al. Fractal dimension as a prognostic factor for laryngeal carcinoma. Anticancer Res. 2005; 25: 2141-4.
6) Ferro DP, Falconi MA, Adam RL, Ortega MM, Lima CP, de Souza CA, et al. Fractal Characteristics of May-Grünwald-Giemsa Stained Chromatin Are Independent Prognostic Factors for Survival in Multiple Myeloma. PLoS One. 2011; 6: e20706.
7) Bedin V, Adam RL, de Sá BC, Landman G, Metze K. Fractal dimension of chromatin is an independent prognostic factor for survival in melanoma. BMC Cancer. 2010; 10: 260.
8) Liliana S, Mircea C F, Carmen P, Daniela C, Corina L G, Stelian S M CTSt. A pilot study on the role of fractal analysis in the microscopic evaluation of colorectal cancers. Rom J Morphol Embryol. 2015; 56: 191-6.
9) Waliszewski P. The Quantitative Criteria Based on the Fractal Dimensions, Entropy, and Lacunarity for the Spatial Distribution of Cancer Cell Nuclei Enable Identification of Low or High Aggressive Prostate Carcinomas. Front Physiol. 2016; 7: 34.
10) Bikou O, Delides A, Drougou A, Nonni A, Patsouris E, Pavlakis K. Fractal dimension as a diagnostic tool of complex endometrial hyperplasia and well-differentiated endometrioid carcinoma. In Vivo (Brooklyn). 2016; 30: 681-90.

11) Adam RL, Silva RC, Pereira FG, Leite NJ, Lorand-Metze I, Metze K. The fractal dimension of nuclear chromatin as a prognostic factor in acute precursor B lymphoblastic leukemia. Cell Oncol. 2006; 28: 55-9.
12) Satoh A. Fractal Analysis of Pit Patterns of Colorectal Epithelial Neoplasia - Qauntification of Pit Patterns and their correlation to Histopathologies -. Niigata Med J. 2005; 119: 464-73.
13) Liebovitch L, Toth T. A fast algorithm to determine fractal dimensions by box counting. Physics Letters A. 1989; 141: 386-90.
14) Russell DA, Hanson JD, Ott E. Dimension of Strange Attractors. Phys Rev Lett. 1980; 45: 1175-8.
15) Cross SS. Fractals in pathology. J Pathol. 1997; 182: 1-8.
16) Lopes R, Betrouni N. Fractal and multifractal analysis: A review. Med Image Anal. 2009; 13: 634-49.
17) Japanthyroid.jp [Internet]. Tokyo: Japan Thyroid Association; c 2019 [cited 2019 Aug 20]. Available from: http://www.japanthyroid.jp/doctor/guidline/japanese.html(cited 2019-8-20).
18) Yoon JH, Yoo JH, Kim EK, Moon HJ, Lee HS, Seo JY, et al. Real-time elastography in the evaluation of diffuse thyroid disease: a study based on elastography histogram parameters. Ultrasound Med Biol. 2014; 49: 2012-9.
19) Loy M, Cianchetti ME, Cardia F, Melis A, Boi F, Mariotti S. Correlation of computerized gray-scale sonographic findings with thyroid function and thyroid autoimmune activity in patients with Hashimoto's thyroiditis. J Clin Ultrasound. 2004; 32: 136-40.
20) Mazziotti G, Sorvillo F, Iorio S, Carbone A, Romeo Mariotti A, et al. Grey-scale analysis allows a quantitative evaluation of thyroid echogenicity in the patients with Hashimoto's thyroiditis. Clin Endocrinol. 2003; 59: 223-9.
21) Ferreira RC, de Matos PS, Adam RL, Leite NJ, Metze K. Application of the Minkowski-Bouligand fractal dimension for the differential diagnosis of thyroid follicular neoplasias. Cell Oncol. 2006; 28: 331-3.
22) Prochazka A, Gulati S, Holinka S, Smutek D. Classification of Thyroid Nodules in Ultrasound Images Using Direction-Independent Features Extracted by Two-Threshold Binary Decomposition. Technol Cancer Res Treat. 2019; 18: 1-8.
23) Lennon FE, Cianci GC, Cipriani NA, Hensing TA, Zhang HJ, Chen CT, et al. Lung cancer-a fractal viewpoint. Nat Rev Clin Oncol. 2015; 12: 664-75.
24) Hayano K, Lee SH, Yoshida H, Zhu AX, Sahani DV. Fractal analysis of CT perfusion images for evaluation of antiangiogenic treatment and survival in hepatocellular carcinoma. Acad Radiol. 2015; 21: 654-60.
25) Merritt CRB. Physics of ultrasound. In: Rumack CM, Wilson SR, Charboneau JW, Levine D, editors. Diagnostic Ultrasound. 4th ed. Philadelphia: Elsevier; 2011. p. 2-33.
26) Muller HW, Schroder S, Schneider C, Seifert G. Sonographic Tissue Characterisation in Thyroid Gland Diagnosis. Klin Wochenschr. 1985; 63: 706-10.
27) Takahashi MS, Moraes PHM, Chammas MC. Ultrasound Evaluation of Thyroiditis: A Review. J Otolaryngol Res. 2019; 2: 127-35.
28) Faggiano A, Del Prete M, Marciello F, Marotta V, Ramundo V, Colao A. Thyroid diseases in elderly. Minerva Endocrinol. 2011; 36: 211-31.
29) Rukhman N, Silverberg A. Thyroid cancer in older men. Aging Male. 2011; 14: 91-8.
30) Havard CWH. The thyroid and aging. Clinics Endocrin Metabol. 1981; 10: 163-78.
31) Metze K, Adam RL, Vido JR, Lorand-Metze IGH. The influence of staining characteristics on nuclear texture features in cytology. Anal Quant Cytol Histol. 2009; 31: 241-6.
32) Normant F, Tricot C. Method for evaluating the fractal dimension of curves using convex hulls. Phys Rev A. 1991; 43: 6518-25.
33) Appleby S. Multifractal characterization of the distribution pattern of the human population. Geogr Anall. 1996; 28: 147-60.
34) Pruess SA. Some Remarks on the Numerical Estimation of Fractal Dimension Fractals in the Earth Sciences. 1st ed. Boston: Springer US; 1995. p. 65-75.
35) Levine RA. Something old and something new: a brief history of thyroid ultrasound technology. Endocr Pract. 2004; 10: 227-33.